



This is the accepted manuscript made available via CHORUS, the article has been published as:

Quadratic Scaling of Intrinsic Gilbert Damping with Spin-Orbital Coupling in $L1_{00}$ FePdPt Films: Experiments and Ab Initio Calculations

P. He, X. Ma, J. W. Zhang, H. B. Zhao, G. Lüpke, Z. Shi, and S. M. Zhou

Phys. Rev. Lett. **110**, 077203 — Published 12 February 2013

DOI: [10.1103/PhysRevLett.110.077203](https://doi.org/10.1103/PhysRevLett.110.077203)

Quadratic scaling of intrinsic Gilbert damping with spin-orbital coupling in L1₀ FePdPt films: Experiments and *ab initio* calculations

P. He^{1,4}, X. Ma², J. W. Zhang⁴, H. B. Zhao^{2,3}, G. Lüpke², Z. Shi⁴, and S. M. Zhou^{1,4}

¹Surface Physics State Laboratory and Department of Physics, Fudan University, Shanghai 200433, China

²Department of Applied Science, College of William and Mary, Williamsburg, Virginia 23185

³Key Laboratory of Micro and Nano Photonic Structures (Ministry of Education) and Department of Optical Science and Engineering, Fudan University, Shanghai 200433, China and

⁴Shanghai Key Laboratory of Special Artificial Microstructure Materials & Technology and School of Physics Science and Engineering, Tongji University, Shanghai 200092, China

The dependence of the intrinsic Gilbert damping parameter α_0 on the spin-orbital coupling strength ξ is investigated in L1₀ ordered FePd_{1-x}Pt_x films by time-resolved magneto-optical Kerr effect measurements and spin-dependent *ab initio* calculations. Continuous tuning of α_0 over more than one order of magnitude is realized by changing the Pt/Pd concentration ratio showing that α_0 is proportional to ξ^2 as changes of other leading parameters are found to be negligible. The perpendicular magnetic anisotropy is shown to have a similar variation trend with x . The present results may facilitate the design and fabrication of new magnetic alloys with large perpendicular magnetic anisotropy and tailored damping properties.

PACS numbers: 75.78.Jp; 75.50.Vv; 75.70.Tj; 75.30.Gw

Ultrafast spin dynamics in ferromagnets is currently a popular topic due to its importance in magnetic information storage and spintronic applications. The real space trajectory of the magnetization precessional switching triggered by magnetic field pulses, femtosecond laser pulses, or spin-polarized currents¹⁻⁶, can be well described by the phenomenological Landau-Lifshitz-Gilbert (LLG) equation that incorporates the Gilbert damping term describing the dissipation of magnetic energy towards the thermal bath⁷. The magnetic Gilbert damping parameter consists of intrinsic homogeneous and extrinsic inhomogeneous damping terms. The latter is caused by nonlocal spin relaxation processes, leading to Gilbert damping enhancement in thin films and heterostructures and can be tuned by artificial substrates, specially designed buffer and coverage layers⁸⁻¹⁰. For magnetic nanostructures, the extrinsic one caused by the dephasing dynamics is found to strongly depend on the element size^{11,12}.

The intrinsic Gilbert damping α_0 has been thought to arise from combined effects of spin orbital coupling (SOC) and electron-phonon interaction, and has been treated by various theoretical models¹³⁻²⁰. In the SOC torque-correlation model proposed by Kamberský, contributions of intraband and interband transitions are found to play a dominant role in low and high temperature (T) regions, respectively^{14,19}. The former/latter term is predicted to decrease/increase with increasing T like the conductivity/resistivity and to be proportional to ξ^3/ξ^2 . Accordingly, α_0 is expected to achieve a minimum at an intermediate T . Since the non-monotonic variation was observed in many *3d* magnetic metals, the effect of electron-lattice scattering has been well demonstrated²¹⁻²³. In contrast, no direct experiments have been reported to rigorously verify the quantitative relationship between α_0 and SOC strength ξ despite many attempts²⁴⁻²⁹. The difficulty lies in the

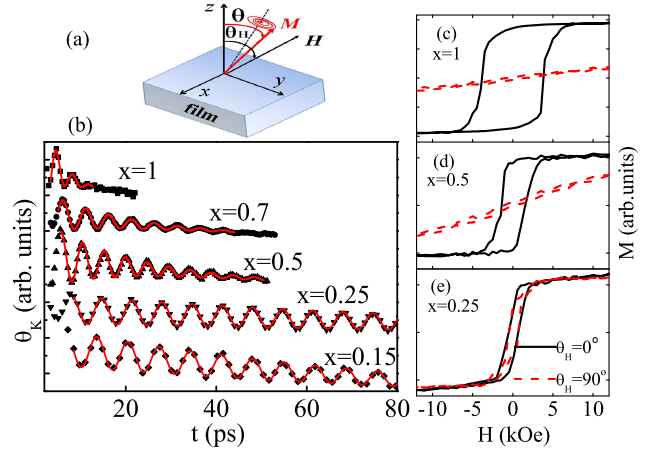


FIG. 1: Schematic illustration of the TRMOKE geometry (a) and measured TRMOKE results (solid symbols) for $x = 0.15, 0.25, 0.5, 0.7,$ and 1.0 with $H = 5$ T and $\theta_H = 45^\circ$ (b). Out-of-plane and in-plane hysteresis loops for $x = 1$ (c), 0.5 (d), and 0.25 (e). In (b) the TRMOKE curves are shifted for clarity and the (red, solid) lines are fit results.

fact that α_0 is also strongly related to other physical parameters such as the density of states $D(E_F)$ at the Fermi surface E_F ^{26,28} and electron scattering time, in addition to ξ , and these leading parameters may change when ξ is tailored by using various metals and alloys. More importantly, there is still a lack of an effective approach for continuously tuning the magnetic damping parameter, although the $D(E_F)$ effect has been demonstrated in Heusler alloys and ferromagnetic semiconductors³⁰⁻³³.

In this Letter, we elucidate the ξ dependence of α_0 by using L1₀ FePd_{1-x}Pt_x (=FePdPt) ternary alloy films

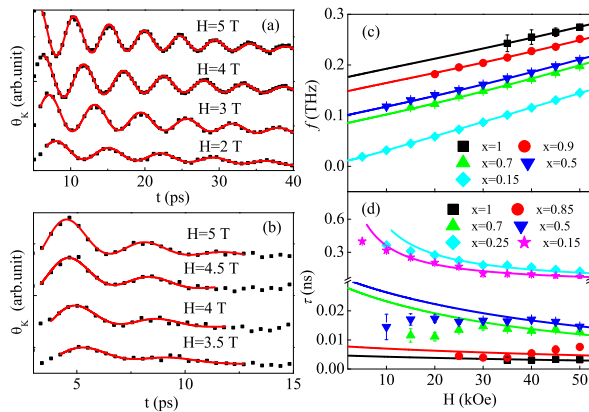


FIG. 2: TRMOKE results for $x = 0.5$ (a) and 1.0 (b) with various magnetic fields and $\theta_H = 45^\circ$. Uniform magnetization precession frequency f (c) and relaxation time (d) as a function of H for typical samples. In (a) and (b) curves are shifted for clarity. In (a), (b), (c), and (d), solid lines refer to fit results.

with varying Pt/Pd ratio. Time-resolved magneto-optical Kerr effect (TRMOKE) measurements show that α_0 can be increased by an order of magnitude when Pd atoms are replaced by Pt because heavier atoms are expected to have a larger ξ^{34} . Our calculations show that α_0 is proportional to ξ^2 at high temperatures because for the present $L1_0$ FePdPt films other parameters are shown to be almost fixed when ξ is artificially modulated by the Pt/Pd concentration ratio. This work will provide a clue to continuously alter the magnetic damping and will also facilitate exploration of new magnetic alloys with reasonably high perpendicular magnetic anisotropy (PMA) and low α .

A series of $L1_0$ FePdPt ternary alloy films with $0 \leq x \leq 1.0$ were deposited on single crystal MgO (001) substrates by magnetron sputtering. The film thickness was determined by X-ray reflectivity (XRR) to be 12 ± 1 nm. The microstructure analysis was performed by X-ray diffraction (XRD). The FePdPt films are of the $L1_0$ ordered structure as proved by the (001) superlattice peak. The chemical ordering degree S can be calculated with the intensity of the (001) and (002) peaks to be about 0.8 for FePt and FePd films. The epitaxial growth was confirmed by a Φ and Ψ scan with 2θ fixed for the (111) reflection of FePdPt films. In order to measure the Gilbert damping parameter α , TRMOKE measurements were performed^{35,36}. A variable magnetic field H up to 5 T was applied at an angle of 45° with respect to the film normal using a superconducting magnet. TRMOKE measurements were performed at 200 K in the geometry depicted in Fig. 1(a). Magnetization hysteresis loops were measured by vibrating sample magnetometer at room temperature. The details of fabrication and measurements are described in supporting materials³⁷.

Figure 1(b) shows the typical TRMOKE results of FePdPt films with various x under $H = 5$ T. The magnetization precession is excited as demonstrated by the oscillatory Kerr signals. Moreover, the magnetic damping is indicated by the decaying precession amplitude with the time delay increasing. In particular, the magnetic damping effect becomes stronger for larger x . As shown in Fig. 1(b), the measured Kerr signal can be well fitted by the following equation³⁵ $\theta_K = a + b * \exp(-t/t_0) + A * \exp(-t/\tau) \sin(2\pi ft + \varphi)$, where parameters A , τ , f and φ are the amplitude, magnetic relaxation time, frequency, and phase of the magnetization precession, respectively. Here, a , b , and t_0 correspond to the background signal owing to the slow recovery process. The relaxation time τ is fitted and found to decrease from about 130.0 to 3.0 (ps) when x changes from 0 to 1.0. Apparently, the magnetic relaxation time can be tuned by the Pt concentration x . Figures 1(c)- 1(e) display the out-of-plane and in-plane magnetization hysteresis loops for $x = 1.0$, 0.5, and 0.25, respectively. As shown in Fig. 1(c), for $x = 1$ ($L1_0$ FePt) the out-of-plane hysteresis loop is almost square-shaped with coercivity $H_C = 3.8$ kOe, indicating the establishment of high PMA. With decreasing x , H_C decreases. For $x = 0.25$ in Fig. 1(e), H_C approaches zero and the out-of-plane and in-plane loops almost overlap with each other, indicating a weak PMA. The PMA therefore increases with increasing x ³⁸. It is shown that the magnetic relaxation time is strongly correlated with the PMA as a function of the Pt concentration x . In experiments, the saturation magnetization for all samples is equal to 1100 emu/cm^3 within 10% relative error, close to the bulk value of $L1_0$ FePt³⁹.

It is essential to uncover the physics behind the x dependence of the magnetic damping effect. Since the extrinsic contribution to α can be suppressed by H , the intrinsic one can be extracted by analyzing the TRMOKE results under different H ^{10,40}. As shown by the TRMOKE results for $x = 0.5$ and 1.0 in Figs.2(a)-2(b), the relaxation time becomes shorter with higher H ⁴¹, accompanied by a shorter precession period. Figures 2(c)-2(d) show the H dependences of the precession frequency f and relaxation time τ for typical samples. Since the dispersion of the precession frequency with H changes significantly with x , the important role of PMA in the precession behavior is clearly demonstrated. It is noted that τ decreases by two orders of magnitude when Pd atoms are all replaced by Pt ones and reaches about 3.0 ps for $x = 1$ ($L1_0$ FePt). Accordingly, only under high H the magnetization precession can be excited because the oscillation period must be much shorter than the relaxation time^{41,42}, as shown in Fig.2(b).

With the magnetic damping parameter $\alpha \ll 1.0$, one can obtain the following dispersion equation $2\pi f = \gamma(H_1 H_2)^{1/2}$, where $H_1 = H \cos(\theta_H - \theta) + H_K \cos^2 \theta$ and $H_2 = H \cos(\theta_H + \theta) + H_K \cos^2 \theta$, $H_K = 2K_U/M_S - 4\pi M_S$ with uniaxial anisotropy constant K_U , gyromagnetic ra-

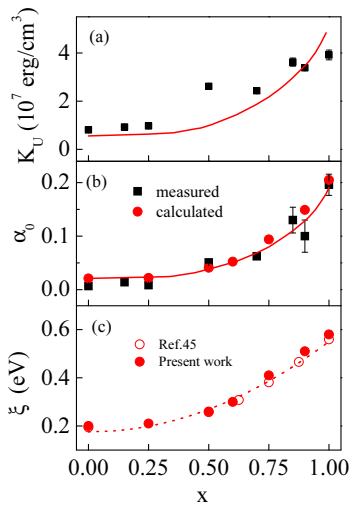


FIG. 3: Measured K_U (a), measured (solid box) and calculated (solid circle) α_0 (b), ξ calculated in this work (solid circle) and in Ref.[45] (open circle) (c) as a function of x . The line in (c) refers to the polynomial fit results. The fitted lines correspond to proportional functions of K_U (a) and α_0 (b) with ξ^2 through the fitted results in (c).

tio γ , and $\theta_H = 45^\circ$. The equilibrium angular position θ of the magnetization satisfies the following equation $\sin 2\theta = (2H/H_K)\sin(\theta_H - \theta)$. The measured field dependence of f can be well fitted by the dispersion relation, as shown in Fig.2(c). With the measured M_S of 1100 emu/cm^3 , the g factor is calculated and found to increase from 2.03 to 2.16 when x changes from 0 to 1.0. A small fraction of the orbital angular momentum is therefore restored by the SOC, close to other independently reported results⁴³. The fitted K_U is shown to increase with increasing x , as shown in Fig.3(a), in agreement with the magnetization hysteresis loops in Figs.1(c)-1(e). For $\alpha \ll 1.0$, α can be in principle extracted by fitting the measured field dependence of τ with $\tau = 2/\alpha\gamma(H_1 + H_2)$ and using the fitted values of g and H_K . As shown in Fig.2(d), however, the fits and experimental data coincide at high fields but seriously deviate at low H . For continuous magnetic films, inhomogeneous effective anisotropy may contribute to the magnetic damping parameter^{8,44}. Since the effect of H_K on the magnetization precession becomes weak with increasing H , the extrinsic contribution and thus α should decrease. The extrinsic one is almost suppressed under high H and accordingly the fitted α value therefore approximately equals the intrinsic α_0 ^{11,41}. The α_0 is found to increase with increasing x , as shown in Fig.3(b).

Spin dependent *ab initio* calculations of the ξ and α_0 in $L1_0$ FePdPt films were performed³⁷. Here, the intrinsic α_0 calculations were concentrated on inter-band transition term with large scattering rate, demonstrating the damping parameter at high temperatures^{14,18}.

As shown in Fig.3(b), calculated and measured results of α_0 are in good agreement. Calculations show that ξ changes from 0.19 to 0.58 (eV) when x varies from 0 to 1.0, as shown in Fig.3(c). The ξ is 0.6, 0.20, and 0.06 (eV) for Pt, Pd, and Fe atoms, respectively^{34,45} and the effect of Fe atoms is negligible compared with those of Pd and Pt atoms. The present results of ξ are in good agreement with previous *ab initio* calculations⁴⁵. Moreover, the $D(E_F)$ is found to change from 2.55 to 2.39 per atom per eV for x varying from 0 to 1.0. From both XRD measurements and theoretical structure analysis of $L1_0$ FePdPt alloys, the lattice constant is found to vary by less than 1.0 percent for different x . Standard electron-phonon scattering calculations were performed with phonon Debye model and static limit of Lindhard's dielectric function. The electron-phonon scattering rate $1/\tau_{e-ph}$ varies from 1.34 to 1.33 ps^{-1} for x changing from 0 to 1.0. Our results show that $1/\tau_{e-ph}$ and $D(E_F)$ are both almost independent of variable x . Figure 4 shows that α_0 is proportional to ξ^2 , where the ξ values at other x are interpolated from the fitted curve in Fig.3(c). Since the lattice constant, $D(E_F)$, Curie temperature, gyromagnetic ratio, electron-phonon scattering rate, and averaged spin, as leading parameters of α_0 ^{19,26,28}, are either experimentally or theoretically shown to be almost constant with x , the increase of α_0 with x is therefore mainly attributed to the larger ξ of Pt atoms. The present work has *rigorously* proven the theoretical prediction of the ξ^2 scaling of α_0 ¹⁴, indicating that α_0 at high temperatures is mainly caused by interband contribution^{14,19}. Moreover, the electronic-scattering-based model of ferromagnetic relaxation is therefore proven to be applicable for α_0 in $L1_0$ FePdPt ternary alloys¹⁴. Further investigation of the magnetization precession at low temperatures will be helpful to get deeper insight into the origin of α_0 ¹⁹.

The results in Figs.3(a) and 3(b) are also helpful to address the correlation between α_0 and PMA. Up to date, the correlation between these two physical quantities is still unclear although this issue has been studied extensively in theory and experiments^{14,15,30-33}. The magnetocrystalline anisotropy is thought to arise from second order energy correction of SOC in the perturbation treatment and is roughly proportional to both ξ and orbital angular momentum when ξ is smaller than the exchange splitting. The orbital momentum in $3d$ magnetic alloys restored by SOC is also proportional to ξ ; therefore PMA is proportional to ξ^2/W with the bandwidth (W) of $3d$ electrons⁴⁶. Since W does not change much with x , the enhanced PMA at high x is attributed to a larger ξ of Pt atoms compared with that of Pd atoms³⁴ and the quadratic scaling law of the PMA with ξ is expected, as proved by the fact that the measured K_U can be fitted by a proportional function of ξ^2 in Fig. 3(a). With the same origin in SOC, it can be easily understood that K_U and α_0 both show similar variation trends as a function of x when other leading parameters except for ξ are almost fixed with varying x in the $L1_0$ FePdPt alloy films.

In summary, we have investigated the magnetiza-

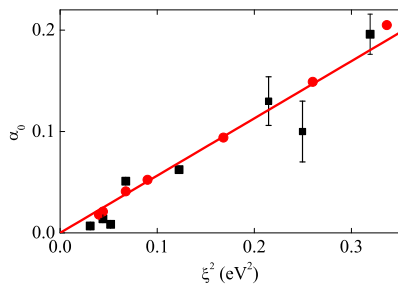


FIG. 4: Experimental (solid squares) and theoretical (solid circles) values of α_0 versus ξ^2 obtained for different x . The solid curve represents a proportional function fit.

tion dynamics in L1₀ FePdPt ternary alloy films using TRMOKE. The intrinsic α_0 can be continuously tuned,

showing an increase with increasing Pt concentration x due to a larger ξ of Pt atoms compared with that of Pd atoms. In particular, the ξ quadratic dependence of α_0 has been rigorously demonstrated in experiments. Moreover, α_0 and PMA show similar trends with Pt concentration. The present experimental results provide deeper insight into the intrinsic damping mechanism in magnetic metallic materials and provide a new clue to explore ideal ferromagnets with reasonably low α_0 and high PMA for applications of magnetic devices.

Acknowledgements This work was supported by the MSTC under grant No. 2009CB929201, (US)DOE grant No. DE-FG02-04ER46127, NSFC under Grant Nos.10974032, 11074044, 51171129, 60908005, and 61222407, NCET(11-0119), Shanghai PuJiang Program (10PJ004), and Shanghai Committee of Science and Technology under grant No.11JC1412700.

- ¹ L. Landau and E. Lifshitz, *Physik Z Sowjetunion* **8**, 153 (1935); T. L. Gilbert, *Phys. Rev.* **100**, 1243(1955);
- ² J. C. Slonczewski, *J. Magn. Magn. Mater.* **159**, L1(1996)
- ³ Th. Gerrits, H. A. M. van den Berg, J. Hohlfeld, and L. Bär *et al*, *Nature (London)* **418**, 509 (2002).
- ⁴ H. W. Schumacher, C. Chappert, R. C. Sousa, and P. P. Freitas *et al*, *Phys. Rev. Lett.* **90**, 17204 (2003).
- ⁵ S. I. Kiselev, J. C. Sankey, I. N. Krivorotov, and N. C. Emley *et al*, *Nature (London)* **425**, 380 (2003).
- ⁶ S. Kaka, M. R. Pufall, W. H. Rippard, and T. J. Silva *et al*, *Nature (London)* **437**, 389(2005)
- ⁷ B. Koopmans, J. J. M. Ruigrok, F. Dalla Longa, and W. J. M. de Jonge, *Phys. Rev. Lett.* **95**, 267207(2005)
- ⁸ R. Urban, G. Woltersdorf, and B. Heinrich, *Phys. Rev. Lett.* **87**, 217204(2001)
- ⁹ D. J. Twisselmann and R. D. McMichael, *J. Appl. Phys.* **93**, 6903(2003)
- ¹⁰ G. Woltersdorf, M. Buess, B. Heinrich, and C. H. Back, *Phys. Rev. Lett.* **95**, 037401 (2005)
- ¹¹ A. Barman, S. Wang, J. Maas, and A. R. Hawkins *et al*, *Appl. Phys. Lett.* **90**, 202504 (2007)
- ¹² A. Laraoui, J. Vénuat, V. Halté, and M. Albrecht *et al*, *J. Appl. Phys.* **101**, 09C105 (2007)
- ¹³ B. Heinrich, D. Fraitová, and V. Kamberský, *Phys. Status Solidi* **23**, 501 (1967).
- ¹⁴ V. Kamberský, *Czech. J. Phys., Sect. B* **26**, 1366(1976); V. Kamberský, *Phys. Rev. B* **76**, 134416(2007)
- ¹⁵ D. Steiauf and M. Fähnle, *Phys. Rev. B* **72**, 064450(2005)
- ¹⁶ A. Brataas, Y. Tserkovnyak, and G. E.W. Bauer, *Phys. Rev. Lett.* **101**, 037207 (2008).
- ¹⁷ M. C. Hickey and J. S. Moodera, *Phys. Rev. Lett.* **102**, 137601 (2009)
- ¹⁸ K. Gilmore, Y. U. Idzerda, and M. D. Stiles, *Phys. Rev. Lett.* **99**, 027204(2007)
- ¹⁹ K. Gilmore, Y. U. Idzerda, and M. D. Stiles, *J. Appl. Phys.* **103**, 07D303(2008)
- ²⁰ H. Ebert, S. Mankovsky, D. Ködderitzsch, and P. J. Kelly, *Phys. Rev. Lett.* **107**, 066603 (2011)
- ²¹ B. Heinrich and Z. Frait, *Phys. Status Solidi* **16**, K11(1966)
- ²² S. M. Bhagat and P. Lubitz, *Phys. Rev. B* **10**, 179(1974)
- ²³ B. Heinrich, D. J. Meredith, and J. F. Cochran, *J. Appl. Phys.* **50**, 7726 (1979)
- ²⁴ S. Ingvarsson, G. Xiao, S. S. P. Parkin, and R. H. Koch, *Appl. Phys. Lett.* **85**, 4995(2004)
- ²⁵ C. Scheck, L. Cheng, I. Barsukov, and Z. Frait *et al*, *Phys. Rev. Lett.* **98**, 117601(2007)
- ²⁶ J. O. Rantschler, R. D. McMichael, A. Castillo, and A. J. Shapiro *et al*, *J. Appl. Phys.* **101**, 033911(2007)
- ²⁷ G. Woltersdorf, M. Kiessling, G. Meyer, and J.-U. Thiele *et al*, *Phys. Rev. Lett.* **102**, 257602(2009)
- ²⁸ A. A. Starikov, P. J. Kelly, A. Brataas, and Y. Tserkovnyak *et al*, *Phys. Rev. Lett.* **105**, 236601(2010)
- ²⁹ A. Rebei and J. Hohlfeld, *Phys. Rev. Lett.* **97**, 117601 (2006)
- ³⁰ S. Mizukami, E. P. Sajitha, F. Wu, and D. Watanabe *et al*, *Appl. Phys. Lett.* **96**, 152502(2010)
- ³¹ S. Mizukami, F. Wu, A. Sakuma, and J. Walowski *et al*, *Phys. Rev. Lett.* **106**, 117201 (2011); M. Oogane, T. Kubota, Y. Kota, and S. Mizukami *et al*, *Appl. Phys. Lett.* **98**, 052501(2011)
- ³² A. Barman, S. Wang, O. Hellwig, and A. Berger *et al*, *J. Appl. Phys.* **101**, 09D102 (2007)
- ³³ S. Pal, B. Rana, O. Hellwig, and T. Thomson *et al*, *Appl. Phys. Lett.* **98**, 082501 (2011)
- ³⁴ K. M. Seemann, Y. Mokrousov, A. Aziz, and J. Miguel *et al*, *Phys. Rev. Lett.* **104**, 076402(2010).
- ³⁵ W. K. Hiebert, A. Stankiewicz, and M. R. Freeman, *Phys. Rev. Lett.* **79**, 1134(1997)
- ³⁶ M. van Kampen, C. Jozsa, J. T. Kohlhepp, and P. LeClair *et al*, *Phys. Rev. Lett.* **88**, 227201(2002)
- ³⁷ See supporting materials at <http://link.aps.org/supplementary/> for details of sample fabrications, microstructure characterization, TRMOKE measurements, and *ab initio* calculations.
- ³⁸ S. Jeong, A. G. Roy, D. E. Laughlin, and M. E. McHenry, *J. Appl. Phys.* **91**, 8813(2002)
- ³⁹ O. A. Ivanov, L. V. Solina, V. A. Demshina, and L. M. Magat, *Fiz. Met. Metalloved.* **35**, 92(1973).

- ⁴⁰ Z. Celinski and B. Heinrich, J. Appl. Phys. **70**, 5935 (1991)
- ⁴¹ J. W. Kim, H. S. Song, J. W. Jeong, and K. D. Lee *et al*, Appl. Phys. Lett. **98**, 092509(2011)
- ⁴² Z. Z. Zhang, B. Y. Cui, G. Z. Wang, and B. Ma *et al*, Appl. Phys. Lett. **97**, 172508 (2010)
- ⁴³ I. V. Solovyev, P. H. Dederichs, and I. Mertig, Phys. Rev. B **52**, 13419(1995)
- ⁴⁴ Y. Tserkovnyak, A. Brataas, and G. E. W. Bauer, Phys. Rev. Lett. **88**, 117601(2002)
- ⁴⁵ P. He, L. Ma, Z. Shi, and G. Y. Guo *et al*, Phys. Rev. Lett. **109**, 066402 (2012)
- ⁴⁶ P. Bruno, Phys. Rev. B **39**, 865(1989)